Spatial Resolution in Micrometric Periodic Assemblies of Magnetotactic Bacteria and Magnetic Nanoparticles

A. J. Moreno[1], E. Gonzalez[2], M. Godoy[3], J. Pettinari[3], P. S. Antonel[4], G. Jorge[1], and V. Bekeris[1]

[1]Laboratorio de Bajas Temperaturas, Departamento de Física, FCEyN, UBA, IFIBA, CONICET, Buenos Aires, Argentina
[2]Departamento de Física, FCEyN, UBA Buenos Aires, Argentina
[3]Laboratorio de Genética y Ecología Microbianas, Departamento de Química Biológica, FCEyN, UBA, Buenos Aires, Argentina
[4]Laboratorio de Arreglos Multisensoriales, Departamento de Química Inorgánica, Analítica y Química Física, FCEyN, UBA INQUIMAE, CONICET, Buenos Aires, Argentina

We developed a simple method for obtaining micro arrays of magnetic nanoparticles using audio tapes. We present spatial micro-arrangements of magnetotactic bacteria (*Magnetospirillum gryphiswaldense*), magnetite (Fe_3O_4) and functionalized cobalt ferrite ($CoFe_2O_4$) nanoparticles. Computer generated square audio waves of different frequencies (100 Hz–10 kHz) were recorded leading to magnetic patterns of different micrometer spatial wavelengths. Drops of aqueous suspensions were deposited on the tapes to control particle density, and bacteria and particles were trapped at locations where magnetic energy is minimized, as observed using conventional optical microscopy after the dispersium medium was evaporated. We discuss the spatial limits of the magnetic nanoparticles and the bacteria assemblies, concluding that cell walls of bacteria inhibit agglomeration and optimize spatial organization.

***Index Terms*—Magnetic nanoparticles, magnetic particle imaging, magnetic tapes, magnetite, microassembly, microorganisms.**

I. Introduction

THE MANIPULATION of magnetic nanoparticles into custom-made structures [1], [2] is particularly promising for applications in spintronics, novel memory devices, and in biology [3]–[5].

We study different types of magnetic particles and *Magnetospirillum gryphiswaldense* magnetotactic bacteria (MTB) interacting with controlled periodic magnetic substrates. The substrates are audio tapes recorded with square audio waves of different frequencies, $100\ \text{Hz} < f < 10$ kHz, that create in-plane periodic magnetic domains of wavelengths between 476 μm to 4.8 μm. The high frequency signals are distorted by the recording mechanism. We found that the high Fourier components are attenuated for frequencies larger than 5 kHz so only the first few harmonics are recorded on the tape. Also, at lower frequencies we found this effect blurs the rising and falling edges of the square wave, producing additional oscillatory signals observed in the particle patterns. The magnetic stray field of periodic domains has been measured and calculated in the past [6] and the magnetic interaction is evaluated below to describe the final position of the particles.

The paper is organized as follows. In Section II, we describe the experimental array and the method used to deposit the particles. Results and discussion are presented in Section III and conclusions are drawn in Section IV.

II. Experiment

The physics of tape recording is well understood [7]. The voltage waveform to be recorded activates a writing head that magnetizes the tape as it moves at constant speed in close contact to it, creating in-plane magnetized domains. In this work, we used computer generated bipolar square wave functions of different fundamental frequencies, and the tape magnetization wavelength is determined by the tape velocity, $v = 48$ mm/s. As frequency is increased, the square signal is distorted because the higher Fourier components are attenuated, and therefore the rising and falling edges become oscillatory. In previous work [6], [8], we have estimated the magnetization $\mathrm{m_0}$ per unit area on each half period and observed by magneto optic technique the stray perpendicular field of tapes [6], [8] in coincidence with calculations described below.

Magnetospirillum gryphiswaldense were grown in flask standard medium for 1 week at 30 °C in anaerobic conditions as described elsewhere [8]. Bacteria were typically 3–9 μm long and contain nanometric particles of magnetite (diameter 14–67 nm) forming chains of approximately 50 elements inside the cells [9].

The $CoFe_2O_4$ nanocrystals were prepared by a chemical coprecipitation method described in [10]. The mean diameter of the prepared nanoparticles was (12 ± 2) nm, as seen by transmission electron microscopy (TEM) micrographs (not shown). The chemical coprecipitation method was also used for the synthesis of magnetite Fe_3O_4 nanoparticles. TEM micrographs (not shown) indicate an average size of (14 ± 2) nm in diameter. Fe_3O_4 nanoparticles are superparamagnetic [8] but $CoFe_2O_4$ nanoparticles are ferromagnetic and form aggregates due to dipole–dipole interactions. Optical inspection indicates that the typical aggregate volume for Fe_3O_4 is similar to a bacterium volume ($\sim 0.125\ \mu\text{m}^3$). $CoFe_2O_4$ aggregates are larger and more difficult to disperse in the liquid medium due to stronger magnetic interactions, so $CoFe_2O_4$ nanoparticles were functionalized using polyaniline [11] in order to decrease the magnetic interactions. The aggregate volume was reduced although aggregates still formed.

The method to create the particle assemblies consists of depositing a drop of an aqueous suspension of magnetic particles

Manuscript received February 15, 2013; revised March 26, 2013, April 12, 2013; accepted April 17, 2013. Date of current version July 23, 2013. Corresponding author: A. J. Moreno (e-mail: amoreno@df.uba.ar).

Color versions of one or more of the figures in this paper are available online at http://ieeexplore.ieee.org.

Digital Object Identifier 10.1109/TMAG.2013.2259224

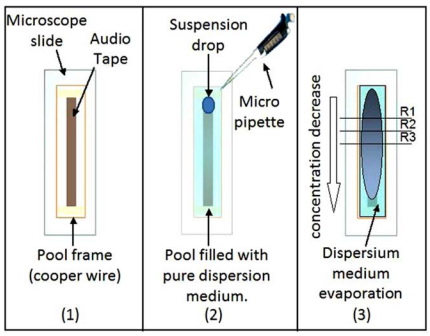

Fig. 1. Schematic view of decoration procedure. (1) Microscope slide with recorded magnetic tape and pool frame. (2) Pool was filled with pure water and a drop of suspension was deposited. (3) Nanoparticles and/or MTB diffused and the dispersion medium evaporated before optical observation. $\mathrm{R_i}$ $(\mathrm{i} = 1 - 3)$ indicate approximately the positions in the decorated tape where photos were taken.

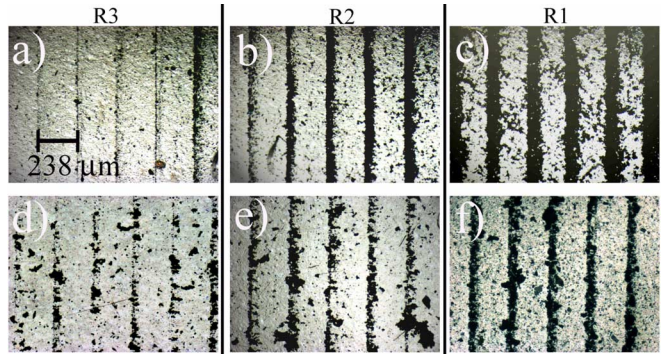

Fig. 2. Gradient of particle concentration. Top row Fe_3O_4 particles; bottom row $CoFe_2O_4$ particles. (c) and (f) Micrographs at (R1); see Fig. 1. panel 3). (b) and (e) Micrographs at R2. (a) and (d) Micrographs at R3. All micrographs are at 100X magnification in a 100 Hz tape.

on top of a recorded audio tape and observing optically the distribution of particles after the dispersion medium evaporates. We denominate this protocol the "decoration" procedure.

Nanoparticle suspensions (Fe_3O_4 and $CoFe_2O_4$) of known concentration were extensively sonicated before a drop was extracted by means of a micro pipette. The particle concentration was difficult to control during decoration due to the different rates of particle precipitation and agglomeration (different rates of precipitation also occurred with MTB suspensions). To solve this difficulty we developed the following procedure: A recorded tape was fixed to a microscope slide with the magnetized side pointing upwards. Then a flexible copper wire was fixed around the recorded tape to form a large "pool" approximately 10 mm wide and 30 mm long, as schematized in Fig. 1 panel 1). The wire was covered with transparent nail polish to seal the pool and then it was filled with ∼0.2 ml of pure water. Then a ∼10 μl drop of suspension, of MTB, Fe_3O_4 or $CoFe_2O_4$ (decorating elements) was deposited using a micro pipette close to one of the narrower edges of the pool, as shown in panel 2). After particle diffusion and precipitation, water was allowed to evaporate. The decorated tapes were observed with a standard Olympus BX60M microscope and a Roper Scientific CoolSnap CF camera recorded the images, which show that particle concentration becomes gradually more diluted towards the opposite pool edge as indicated in panel 3) by an arrow.

To illustrate decorations for different particle densities, micrographs were analyzed at three different positions within each tape, indicated with lines labeled R1-R3 in Fig. 1 panel 3). This procedure was repeated for recorded tapes with different frequencies. Each micrograph was analyzed using Photoshop and ImageJ to calculate the percentage of the micrograph surface covered with particles (e.g., black pixels). Assuming that the particles formed a uniform layer, particle concentration was determined as the quotient of black pixels over total pixels.

III. Results and Discussion

The perpendicular (B_z) and parallel (B_y) magnetic field components close to the surface of an infinite strip magnetized with period l, where the magnetic moment per unit length is $\pm m_0 \mathrm{e_y}$, are given by the following:

$$B_z = \frac{4\pi}{l}\mu_0 \sum_{n=0}^{\infty}\left[na_n \cos\left(\frac{2\pi n}{l}y\right) - nb_n \sin\left(\frac{2\pi n}{l}y\right)\right] \quad (1)$$

$$B_y = -\frac{4\pi}{l}\mu_0 \sum_{n=0}^{\infty}\left[na_n \sin\left(\frac{2\pi n}{l}y\right) + nb_n \cos\left(\frac{2\pi n}{l}y\right)\right] \quad (2)$$

where $\mathrm{a_n}$ and $\mathrm{b_n}$ are the magnetization Fourier expansion coefficients. The force on a particle of moment m is given by the following:

$$F = -(m \cdot \nabla)B. \quad (3)$$

As m is parallel to B, the particles are then forced towards the peaks in B_z along $\boldsymbol{y}$, and against the tape surface, remaining attached. See further analysis in [6] and [8].

We now present the micrographs of the decorations on tapes recorded at different frequencies and with different particles.

In Fig. 2, we show evidence of concentration variation along a 100 Hz recorded tape, decorated with Fe_3O_4 [panels a), b), and c)] and $CoFe_2O_4$ [panels d), e), and f)]. Panels in each row correspond to three different positions: ∼1.5, ∼1.0 and ∼0.5 cm away from the suspension drop, indicated in Fig. 1 panel 3) as R3, R2, and R1. The average distance between lines (∼238 μm) corresponds, as expected, to half wavelength for 100 Hz, but the line width along the pattern clearly becomes narrower as the distance to the drop increases and the particle concentration decreases. Particle diffusion and precipitation determine the variation in concentration.

Note that ferromagnetic $CoFe_2O_4$ particles [8] tend to aggregate even at low concentrations [see Fig. 2(d)] forming patterns with irregular line widths reducing the uniformity of the patterns. In contrast, superparamagnetic magnetite and bacteria [8] [see Fig. 3(a) and (b)] do not aggregate, leading to more homogeneous line widths.

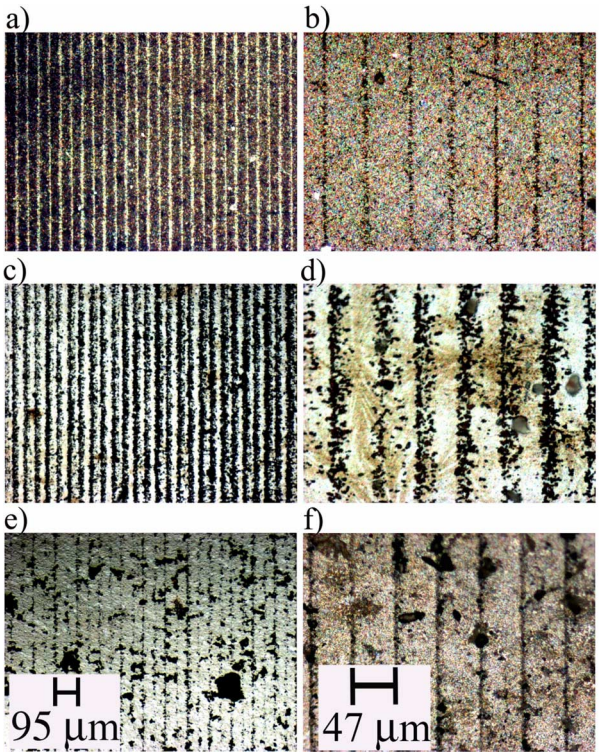

Fig. 3. Decorations using a 500 Hz tape. First row: MTB (a) 50X (b) 200X. Second row: Fe_3O_4 (c) 50X (d) 200X. Third row: $CoFe_2O_4$ (a) 50X, (b) 200X.

We performed decorations on tapes recorded at different frequencies. Line width, uniformity of the particle concentration along the line and line separation, as well as the low wavelength limit of spatial decoration, were analyzed. Micrographs (50X and 200X) in Fig. 3 show typical decorations with bacteria (top), Fe_3O_4 (middle) and $CoFe_2O_4$ particles (bottom panels), for tapes recorded with 500 Hz square waves. The observed line separation is $\sim$47 μm, as expected.

Fig. 4 shows the (average) distance between lines [panel a)] and the average line width [panel b)] as a function of frequency for the three types of decorating elements at similar particle concentration. The periodicity of the pattern is independent of the particles and is in excellent accordance with the calculated periodicity. The line width is related to the magnetic characteristic behavior of each type of particle. Superparamagnetic Fe_3O_4 particles are initially well dispersed in the medium, and interparticle interactions become dominant only near the magnetized surface of the tape, producing the widest lines. On the other hand, ferromagnetic $CoFe_2O_4$ particles due to their ferromagnetic characteristics tend to aggregate, so there are very few single particles (or small aggregates) dispersed on the medium. The line width is narrower and large aggregates are observed. Finally, bacteria are well dispersed and produce the narrowest lines probably due to the cell membranes that reduce particle interactions and avoid agglomeration.

At higher frequencies decorations show patterns with line separations that match a complete wavelength. As it can be seen in Fig. 5, patterns show approximately 9.8 μm line separation for $f = 5$ kHz.

Panel a) shows MTB decoration as dark lines. In panel b) we can distinguish between the magnetized area of the tape which

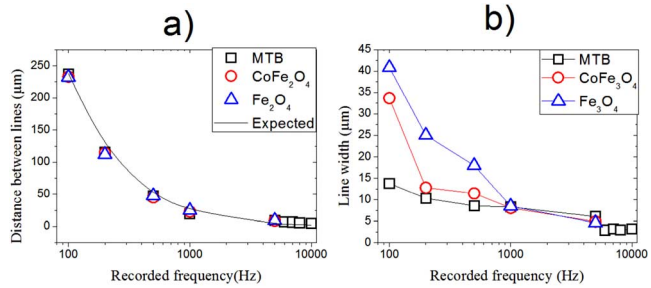

Fig. 4. Comparison between different decorating elements: (a) Distance between lines and (b) line width, for different recorded frequencies.

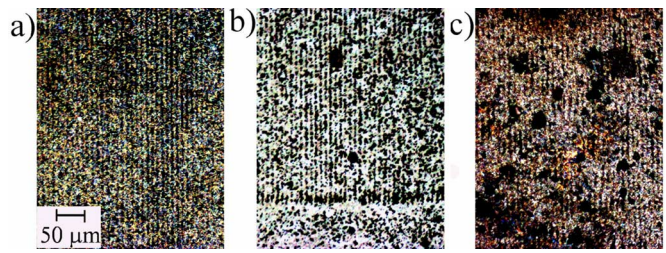

Fig. 5. Decorations using a 5 kHz tape. (a) MTB, (b) Fe_3O_4 and (c) $CoFe_2O_4$. All 100X images.

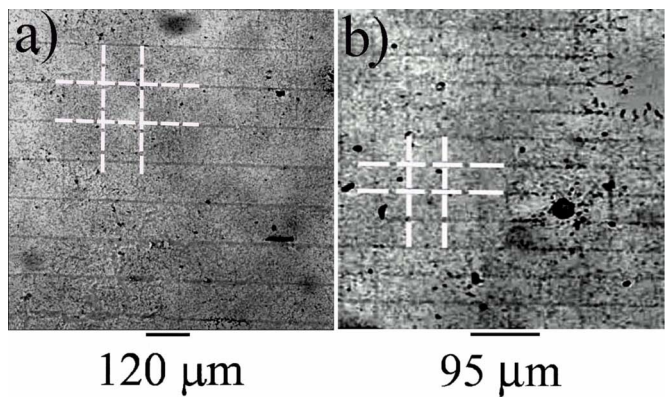

Fig. 6. Double decorations using MTB forming square patterns. (a) 200 Hz tape. (b) 500 Hz tape. Dark (nonstraight) lines are artifacts. White dashed lines are a guide to the eye.

shows decorated lines of Fe_3O_4 and below the nonmagnetized area shows a random distribution of particles. Some aggregates can be seen. Panel c) shows $CoFe_2O_4$ decoration where faint decorated lines can be seen and there are several large aggregates, even after sonication.

For higher frequencies, even due to the harmonic attenuation, we were able to produce patterns using MTB with line distances of 7.5, 6.8 and 5.4 μm corresponding to 6, 7 and 8 kHz frequencies, but no clear pattern was observed when Fe_3O_4 or $CoFe_2O_4$ were used. These patterns also show lengths that correspond to a complete wavelength of the recorded wave as it is shown in Fig. 4 panel a). The reason for this is still unclear. No patterns were observed for frequencies higher than 9 kHz that correspond to a magnetic domain size smaller than the average bacterium or particle aggregate size.

Finally, we were able to produce more complex patterns with MTB. The tape was fixed to the microscope slide with its magnetized face pointing downwards, towards the glass slide and

the suspension was slided in between. Once dry, the tape was removed and a similar tape was fixed again rotating it 90° and the procedure was repeated. We could obtain MTB cells attached to the slide showing a square pattern as shown in Fig. 6 for a 200 Hz tape [panel a)] and 500 Hz [panel b)].

IV. Conclusion

We have studied micrometric periodic assemblies of magnetotactic bacteria (*Magnetospirillum gryphiswaldense*), cobalt ferrite ($CoFe_2O_4$) and magnetite (Fe_3O_4) nanoparticles. Assemblies were generated using audio tapes, previously recorded with computer generated bipolar square audio waves of frequencies between 100 Hz and 5 KHz. The particles form a pattern of parallel lines with wavelengths between 238 and 4.8 μm, located at the tape's magnetic domain walls.

The patterns were observed with an optical microscope and micrographs were analyzed, particularly the line separation, width and width regularity and we found that the cobaltite particles, although functionalized, showed strong particle aggregation reducing the quality of the patterns. Magnetite particles, on the other hand, decorated satisfactorily the tapes but the highest definition was obtained for bacteria. We conclude that the bacteria membranes avoid aggregation and the internal magnetite chains align efficiently with magnetic field. Future work is required to attach particle patterns to different surfaces.

Acknowledgment

This work was supported in part by PICT 2008 Number: 753 ANPCyT and UBACyT EX 661.

References

[1] V. F. Puntes *et al.*, "Colloidal nanocrystal shape and size control: The case of cobalt," *Science*, vol. 291, no. 5511, pp. 2115–2117, Mar. 2001.

[2] S. Malynych *et al.*, "Fabrication of two-dimensional assemblies of Ag nanoparticles and nanocavities in poly(dimethylsiloxane) resin," *Nano Lett.*, vol. 1, no. 11, pp. 647–649, Sep. 2001.

[3] C. T. Black *et al.*, "Spin-dependent tunneling in self-assembled cobalt-nanocrystal superlattices," *Science*, vol. 290, no. 5494, pp. 1131–1134, Nov. 2000.

[4] S. Sun *et al.*, "Monodisperse FePt nanoparticles and ferromagnetic FePt nanocrystal superlattices," *Science*, vol. 287, no. 5460, pp. 1989–1992, Mar. 2000.

[5] U. Häfeli *et al., Scientific and Clinical Applications of Magnetic Carriers*. New York, NY, USA: Plenum, 1997.

[6] H. Ferrari *et al.*, "Magneto-optic imaging: Normal and parallel field components of in-plane magnetized samples," *J. Magn. Magn. Mater.*, vol. 313, no. 1, pp. 98–109, June 2007.

[7] R. C. O'Handley*, Modern Magnetic Materials, Principles and Applications*. New York, NY, USA: Wiley, 2000.

[8] M. Godoy *et al.*, "Micrometric periodic assembly of magnetotactic bacteria and magnetic nanoparticles using audio tapes," *J. Appl. Phys.*, vol. 111, pp. 44905–44911, Feb. 2012.

[9] C. Moisescu, "Controlled biomineralization of magnetite (Fe_3O_4) by Magnetospirillum gryphiswaldense," *Mineralogical Mag.*, vol. 72, no. 1, pp. 333–336, Feb. 2008.

[10] Y. I. Kim *et al.*, "Synthesis and characterization of $CoFe_2O_4$ magnetic nanoparticles prepared by temperature-controlled coprecipitation method," *Physica B*, vol. 337, no. 1–4, pp. 42–51, Sep. 2003.

[11] P. S. Antonel *et al.*, "Anisotropy and relaxation processes of uniaxially oriented $CoFe_2O_4$ nanoparticles dispersed in PDMS," *Physica B*, vol. 407, no. 16, pp. 3165–3167, Aug. 2012.